

## Experimental Investigation on Adsorption Capacity of a Variety of Activated Carbon/Refrigerant Pairs

Ahmed N. Shmroukh\*, Ahmed Hamza H. Ali\*\*, Ali K. Abel-Rahman\* and S. Ookwara \*\*

\*(Energy Resources Engineering Department, Egypt- Japan University of Science and Technology E-JUST, New Borg Elarab, Alexandria 21934, Egypt)

\*\* (Mechanical Engineering Department, Faculty of Engineering, Assiut University, Assiut, Egypt)

\*\*\* (Department of Chemical Engineering, Graduate School of Science & Engineering, Tokyo Institute of Technology, Tokyo 152-8552, Japan)

### ABSTRACT

This study aims to develop a device with minimum heat and mass transfer limitations between adsorbent and adsorbate, and subsequently to obtain practically applicable adsorption capacity data. Also, 5 kW adsorption chillers (evaporators, condensers and adsorbers) are designed based on the experimental output data of the whole tested pairs. A finned-tube heat exchanger was employed and installed at the center adsorber, and each employed adsorbent was immobilized on its surfaces by using an adhesive agent. A variety of pairs: are activated carbon powder (ACP)/R-134a, ACP/R-407c, ACP/R-507A, activated carbon granules (ACG)/R-507A, ACG /R-407c and ACG /R-134a, were examined at different adsorption temperatures of 25, 30, 35 and 50°C. It was found that, at the adsorption temperature of 25°C the maximum adsorption capacity was 0.8352 kg kg<sup>-1</sup> for ACP/R-134a, while at the adsorption temperature of 50°C the maximum adsorption capacity was 0.3207 kg kg<sup>-1</sup> for ACP/R-134a. Therefore, the ACP/R-134a pair is highly recommended to be employed as adsorption refrigeration working pair because of its higher maximum adsorption capacity higher than the other examined pairs.

**Keywords** - Adsorption; Adsorbent/Adsorbate Pairs; Adsorption Capacity; Refrigeration

### I. Introduction

The development of adsorption refrigeration technology is recently paid much attention. It was favorably argued that such sorption systems were quiet, long lasting, cheap to maintain and environmentally benign [1]. A vital and important component in the adsorption refrigeration system is adsorption refrigeration working pair, of which the developments directly lead to the performance improvement of the adsorption refrigeration systems.

Therefore, the utilization of adsorption refrigeration technology is a first step toward developing an energy efficient and environmental friendly air conditioning and refrigeration systems. The second step is to employ an effective refrigerant with the solid adsorbent, which has lower environmental impact with higher adsorption capacity than the available pairs. The adsorption cooling and refrigeration systems have the advantages of being free of moving parts, efficiently driven by low-temperature waste heat or renewable energy sources and do not require any synthetic lubricants [2]. Askalany et al. [3] presented a review on adsorption cooling systems with adsorbent pairs of activated carbon (AC) with ammonia, methanol, ethanol, hydrogen, nitrogen and diethyl, ether pitch based AC (Maxsorb III) with R134a, R507A and n-butane and AC/CO<sub>2</sub> respectively. Their review

showed that the highest adsorption capacity of 0.055 g g<sup>-1</sup> at 30 °C and 6 bar for AC/hydrogen pair, 0.75 g g<sup>-1</sup> at -4 °C for activated carbon fibers/nitrogen pair, 0.00139 g g<sup>-1</sup> at 50 °C and 0.1 bar for AC/diethyl ether, 2 g g<sup>-1</sup> at 30 °C and 8 bar for AC/R134a, 1.3 g g<sup>-1</sup> at 20 °C for AC/R507a, 0.8 g g<sup>-1</sup> at 35 °C and 2.3 bar for AC/n-butane and 0.084 g g<sup>-1</sup> at 30 °C and 1 bar for AC/CO<sub>2</sub> pair respectively. They also concluded that the maximum Coefficient of Performance (COP) of the cooling systems was 0.8 for AC/ethanol pair and the performances possible adsorption cooling systems with carbon are still not satisfactory. In their review, it can be noted that the refrigerants of R134a and R507a have high global warming potential (GWP), while n-butane, hydrogen, methanol, ethanol and diethyl ether are highly flammable gases, and further, ammonia is a highly toxic refrigerant. Solmus et al. [4] have successfully conducted a numerical investigation of coupled heat and mass transfer inside the adsorbent bed of a silica gel/water adsorption cooling unit, by employing the local volume averaging method. They developed a transient one-dimensional local thermal non-equilibrium model, which accounts for both internal and external mass transfer resistances. Askalany et al. [5] have carried out an experimental study on adsorption-desorption characteristics of granular activated carbon/R134a pair. Throughout their

experiments the temperature of the pairs was about 25 °C. Thier experimental results [5] showed that an increase in the adsorbent temperature of the adsorbent leads to a decrease in the maximum adsorption capacity to 0.53 kgR134a kgcarbon<sup>-1</sup> at 60°C in a period of 450 s. The maximum adsorption capacity was found to be 1.68 kgR134a kgcarbon<sup>-1</sup> at 25°C after 1000 s. They also concluded that the granular activated carbon and R134a could be used as an adsorption pair in an adsorption cooling system.

Shmroukh et al. [6] made comparison and gave summary of the state-of-the-art in the application of the adsorption refrigeration working pairs from both classical and modern adsorption pairs. They reported that the maximum adsorption capacity for the classical working pairs was 0.259 kg kg<sup>-1</sup> for AC/methanol while that for the modern working pairs was 2 kg kg<sup>-1</sup> of maxsorb III/R-134a. They also concluded that, the performances of existing adsorption working pairs in adsorption cooling systems are still needs further to be enhanced while the development of novel adsorption pairs having higher sorption capacity with low or no impact on environmental is necessary, to build an adsorption chiller that is compact, efficient, reliable and long life performance adsorption chiller. Moreover, future researches need to be focused on designing the adsorption system that provide efficient heating and cooling for the adsorbent materials by immobilizing the adsorbent material over heat exchanger surface, to allow good heat and mass transfer between the adsorbent and the refrigerant.

In the literature, it can be seen that all the experimental studies on adsorption capacity experiments were carried out on packed bed adsorbers, which could have dead zones inside and resultantly lacking efficient heat and mass transfer. Since such experiments with packed bed could produce inapplicable data, for example, very high values of adsorption pairs capacity which deviate from the real adsorption refrigeration systems. Therefore, the present study focuses on developing a device with minimum heat and mass transfer limitations between adsorbent and adsorbate to obtain practically applicable adsorption capacity data. For this purpose, a finned-tube heat exchanger was employed as a main part located at the center of the adsorber and adsorbate was immobilized over its surface by using adhesive agent. The main objective of the present experimental study is to experimentally evaluate the maximum adsorption capacity of six different adsorption refrigeration working pairs. The pairs of activated carbon powder (ACP)/R-134a, ACP/R-407c, ACP/R-507A, activated carbon granules (ACG)/R-507A, ACG/R-407c and ACG/R-134a, were examined at different adsorption temperatures of 25, 30, 35 and 50 °C.

## II. Experimental Setup, Measurements, Procedures, Data Reduction and Error Analysis

### 2.1 Experimental Setup

A detailed schematic diagram of the test facility with the adsorber (adsorbent tank) heat transfer core is presented in Fig. (1). The test facility mainly consists of adsorber, refrigerant tank, water tank, vacuum pump and piping system.

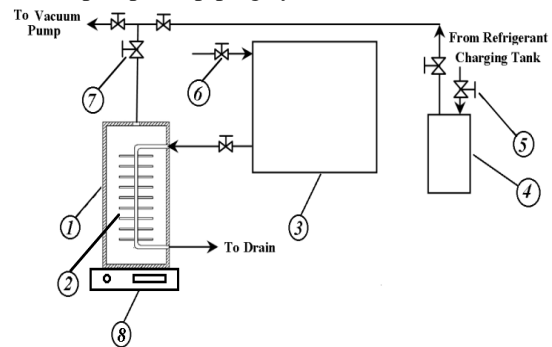
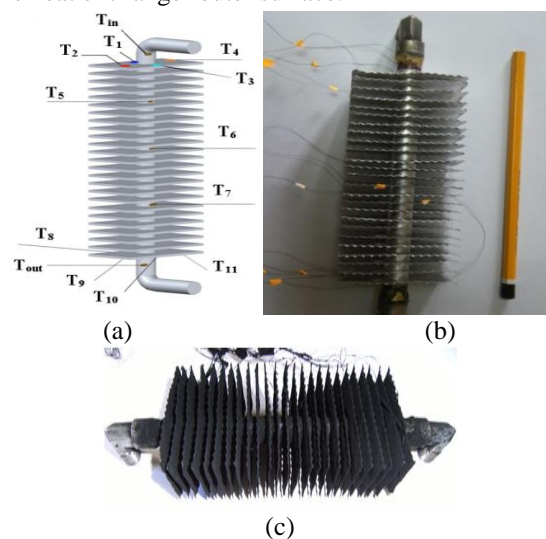


Fig.1: Schematic diagram of the experimental setup of this study, 1) Adsorber, 2) Heat exchanger core, 3) Cooling and heating Water tank, 4) Refrigerant container, 5) Refrigerant charging valve, 6) Water flow control valve, 7) Refrigerant charge/discharge control valve, 8) Electronic balance.

1) Adsorber, 2) Heat exchanger core, 3) Cooling and heating Water tank, 4) Refrigerant container, 5) Refrigerant charging valve, 6) Water flow control valve, 7) Refrigerant charge/discharge control valve, 8) Electronic balance.

The adsorber outer frame is a 2mm thickness galvanized steel tank with dimensions of 7\*5\*23 cm. It is insulated by a 2.5 cm thickness glass wool and foam insulators, and it contains the adsorbent heat and mass transfer core that shown in Fig. (2). The adsorbent heat and mass transfer core is a rectangular aluminum fin and tube heat exchanger with a copper tube and the adsorbent material is immobilized over the heat exchanger outer surface.





(d)

Fig.2: Heat exchanger core assembly (a) temperature measuring points, (b) Photograph before adhesive the adsorbent, (c) Photograph after adhesive the activated carbon powder and (d) Photograph after adhesive the granular activated carbon.

The refrigerant container is a 2mm thickness galvanized steel tank with 10\*10\*20 cm in dimension, the refrigerant charging valve is welded to its top. The tank is insulated by a 2.5 cm thickness glass wool insulator. The Charged refrigerant is from DuPont company refrigerant (canned in Egypt by Rizk Brothers company), the refrigerant properties extracted from tables downloaded from the official website of DuPont company.

The water tank is a 2mm thickness galvanized steel tank with 30\*30\*30 cm in dimension with its cover. It is equipped by a water heater and a thermostat. Cooling and heating water is stored in this tank, to initiate the adsorption and desorption processes. The tank is insulated by a 2.5 cm thickness glass wool insulator. The flowing water temperature is adjusted by a thermostat ranging from 0 °C to 200 °C, with uncertainty of  $\pm$  (0.625% of full scale), it is connected by a contactor to connect and separate the heating coil of 1 kW which fixed at the bottom of the water tank at the required temperature. All the system main components and pipes are insulated by glass wool and insulation foam.

The adsorber is vacuumed by a vacuum pump that is a single-phase RV3 type. This vacuum pump used for vacuuming the system before each adsorption experiment, preventing air presence in the system, to assure that the whole gas in the system is the refrigerant only.

## 2.2 Measurements

In this section a brief description of the instruments used for measuring the temperature, flow rate and pressure are given. All temperatures have been measured by using type T thermocouple (copper, constantan). The voltage output was introduced to a data acquisition device (NEC, DC6100 model) having a maximum of 60 channels, which by turn is connected to a computer for controlling and recording the measured temperature data of measuring points at the same time. Two sizes of thermocouple wires were used; the first size is a 0.1 mm in diameter, which has the junction in contact with the component which temperature is to be measured. The second type is an extension thermocouple wire (Type T) of diameter 0.32 mm,

used to connect the 0.1 mm wire diameter thermocouple some distance away from the component, to keep the splicing junction from being heated using the method used by Ali and Hanaoka [7], which might results in secondary effects that change the temperature reading to the data acquisition device.

All thermocouple junctions had uncertainty of  $\pm$  (0.05% of reading +0.5 °C), these thermocouple junctions made by removing the insulation layer by using fine sanding sheet then twisting the wire ends, then the junctions were connected to the needed measuring points by a very thin adhesive epoxy layer.

The refrigerant pressure was measured by a pressure gauge fixed on the top of the adsorber. The range of this gauge was from -1 to 15 bar absolute, with uncertainty of  $\pm$ 0.25 bar or  $\pm$  (0.833% of full scale).

The mass of the refrigerant entering the adsorbent tank is measured by an electronic balance of 10 kg maximum reading and 0.1g sensitivity, with uncertainty of  $\pm$  0.1g or  $\pm$  (0.001% of full scale).

The volume flow rate of the water exiting from water tank to the adsorbent tank is adjusted to be (0.33 l min<sup>-1</sup>), it is measured by laboratory graded glass bottle (500 ml with 5 ml minimum scale), with uncertainty of  $\pm$  5ml or  $\pm$  (1% of full scale) and stop watch.

## 2.3 Experimental procedures

For all experiments, the following procedure was followed:

1. All the 16 points thermocouples (Type T) are connected by plugs and connectors to the same type leading wires to the data logger.
2. The whole system is evacuated (charging tank, adsorbent tank and piping system) by a vacuum pump to the minimum possible vacuum pressure (25-30 kPa). The adsorber weight is recorded after this step.
3. The target refrigerant for the experiment is charged to the refrigerant container by the charging valve at the top of the container, this container is weighted during charging process until charging 100 g of refrigerant.
4. The charging valve is then closed tightly to prevent refrigerant leakage.
5. The adsorbent tank pressure is measured by the pressure gauge.
6. The mass of the refrigerant entered the adsorbent tank is measured by the electronic balance.
7. The flow rate of water exiting from water tank to the adsorbent tank is measured by laboratory graded glass bottle.
8. The water tank is filled to a fixed level then its valves are closed and the heating process takes place to the required temperature. After that, inlet valve to water tank and exit valve to

adsorbent tank are opened to the specific water flow rate.

9. The electronic balance is operated and the data logger is connected to the computer to present the data, and the reading interval is set to be every 60 sec. This step is continues until both the balance and thermocouples readings are stable and reach steady state.
10. For the adsorption experiments, the refrigerant container valve is slightly opened then the adsorption process readings are started until the balance reading reach to a constant value. This means the adsorption equilibrium or the adsorbent material cannot adsorb more refrigerant. Then the adsorbent tank is evacuated by the vacuum pump to draw out all un-adsorbed refrigerant mass, which was fills the adsorbent tank internal space. This to ensure that there is no refrigerant mass inside the tank except the adsorbed refrigerant quantity. Then the flexible pipe which fixed at the top of the tank is disconnected and the adsorber tank is weighted by the balance. The weight difference between step 2 and this step reading is considered as the exact adsorbed refrigerant quantity. Then the flexible pipe is reconnected and evacuated before open the adsorbent tank valve to reject air, then the valve is opened to be ready for desorption experiment.
11. For the desorption experiment, the refrigerant will return back to its tank by heating the adsorbent. This process is continued until all the adsorbed refrigerant is desorbed from the adsorbent tank and the balance reading reach to be stable and fixed value that nearly equal or a little bit more than the adsorption experiment initial reading. This slightly higher is due to the residual refrigerant in adsorbent pores (hysteresis) which is difficult to rejected by desorption only but need vacuum process.
12. The adsorbent tank valve is closed and the flexible houses are disconnected and the tank is left until reach stable weight reading. Finally, the flexible houses are reconnected and evacuated before opening the adsorbent tank valve in order to reject air. After that, the valve is opened and the test rig is ready for a new experiment.
13. The number of performed adsorption and desorption experiments were 50 (20 adsorption experiments and 30 desorption experiments). The controlled variable in these experiments were the adsorption and desorption temperatures. The adsorption temperatures were 25 °C, 30 °C, 35 °C and 50 °C while the desorption temperatures were 70 °C, 80 °C and 85 °C respectively. The adsorption and desorption conditions chosen to nearly simulate the actual operating conditions in the practical adsorption

refrigeration systems.

The activated carbon powder adsorbent (Norit SA SUPER) used in the experiments was provided by Norit Nederland B.V. Company [Norit Data Sheets]. It was with an extra fine particle size and it was produced by steam activation of dedicated vegetable raw materials. The quantity of activated carbon powder adsorbent used in the experiments was 44.9 g. Its characteristics are summarized in the following table 1: The granular activated carbon adsorbent (Norit GCN 1240) used in the experiments was provided by Norit Nederland B.V. Company [Norit Data Sheets]. It was produced from coconut shells by steam activation. The quantity of granular activated carbon adsorbent used in the experiments was 139.6 g. Its characteristics are summarized in the following Table 2:

Table 1. Activated carbon powder characteristics

Total surface area	3150	m <sup>2</sup> g <sup>-1</sup>
Apparent density	250	m <sup>3</sup> kg <sup>-1</sup>
Average particle size	5	µm

Table 2. Granular activated carbon characteristics

Total surface area	1150	m <sup>2</sup> g <sup>-1</sup>
Apparent density	510	m <sup>3</sup> kg <sup>-1</sup>
Average particle size	0.6	Mm

The refrigerants which used with this adsorbent were:

1. R-134a which is a Hydrofluorocarbon (HFC), its GWP (global warming potential) is 1300 and it has zero ODP (ozone depletion potential) [8].
2. R-507A which is an Azeotropic mixtures, it consists of two refrigerants (HFC-143a 50% and HFC-125 50% by weight) having different properties but behaving as a single substance, its GWP (global warming potential) is 3300 and it has zero ODP (ozone depletion potential) [8].
3. R-407c which is a Nonazeotropic mixtures, it consists of three refrigerants (HFC-32 23%, HFC-125 25% and HFC-134a 52% by weight) having different volatiles, its GWP (global warming potential) is 1526 and it has zero ODP (ozone depletion potential) [8].

#### 2.4 Data Reduction

Refrigerant adsorbed mass is obtained from simple subtraction equation, which was used to determine the mass of the adsorbed refrigerant in adsorption capacity experiment of certain adsorption pair, the initial mass of the adsorption bed subtracted from the final mass of the whole adsorption bed after each run as follows.

$$m_{Ref} = m_{Bed} - m_{Initial} \quad (1)$$

Where  $m_{Ref}$  is the adsorbed refrigerant in kg,  $m_{Bed}$  is the final adsorption bed mass after each run in kg and  $m_{Initial}$  is the initial mass of the adsorption bed before the experiment in kg.

Adsorption pairs capacity is obtained from simple dividing equation to determine the adsorption capacity of each adsorption pair, as the mass of the adsorbed refrigerant in the adsorbent material divided by the mass of the adsorbent as follows.

$$X = \frac{m_{Ref}}{m_{ads}} \quad (2)$$

Where X is the adsorption capacity of the tested working pair in  $kg_{Ref} kg_{ads}^{-1}$ ,  $m_{Ref}$  is the mass of the adsorbed refrigerant in kg and  $m_{ads}$  is the initial mass of the adsorbent in the adsorption bed in kg.

### 2.5 Adsorption Chiller Design

A 5 kW adsorption chiller is designed based on the experimental output data. The three main components which are the condenser, the evaporator and the adsorber designed based on the following steps.

#### 2.5.1 Condensers and Evaporators Design

The previously mentioned equations in chapter three are the needed equations for designing the shell and tube condensers and evaporators of the 5 kW adsorption chiller, for the whole tested six pairs, assuming that the condensers and evaporators temperatures are 40 °C and 10 °C respectively. Using the same concept and steps used in chapter three, assuming that the condenser cooling water inlet temperature is 25 °C and cooling water outlet temperature is 35 °C, and the evaporator chilled water inlet temperature is 22 °C and chilled water outlet temperature is 12 °C, the whole output data for designing the condensers and the evaporators of the experimentally tested adsorption pairs for chiller with 5 kW cooling capacity, a reference SorTech chiller with 15 kW cooling capacity and a reference SorTech chiller with 5 kW cooling capacity, are shown in tables 3 & 4 respectively.

\*For condenser: The condensing power can be calculated from the following equation

$$\dot{Q}_{Cond} = \dot{m}_{CW} * C_{p_{CW}} * \Delta T_{CW} = \dot{m}_{Ref} * (h_1 - h_2) = U_{cond} A_o \Delta T_{LMTD_{Cond}} \quad (3)$$

Where  $\dot{Q}_{Cond}$  is the condenser load in kW,  $\dot{m}_{CW}$  is the condenser cooling water mass flow rate kg/s,  $\Delta T_{CW}$  is the condenser cooling water temperature difference in K,  $\dot{m}_{Ref}$  is the refrigerant mass flow rate kg/s,  $U_{A_o}$  is the overall thermal conductance in W/K and  $\Delta T_{LMTD_{Cond}}$  is the logarithmic mean temperature difference in K. Assuming that cooling water inlet temperature is 25 °C and cooling water outlet temperature is 35 °C.

\*For evaporator: The refrigeration power or the cooling capacity can be calculated from the following equation

$$\dot{Q}_{ev} = \dot{m}_{ChW} * C_{p_{ChW}} * \Delta T_{ChW} = \dot{m}_{Ref} * (h_4 - h_3) = U_{ev} A_o \Delta T_{LMTD_{ev}} \quad (4)$$

Where  $\dot{Q}_{ev}$  is the evaporator cooling load in kW,  $\dot{m}_{ChW}$  is the chilled water mass flow rate kg/s,  $\Delta T_{ChW}$  is the evaporator chilled water temperature difference in K. Assuming that chilled water inlet temperature is 22 °C and chilled water outlet temperature is 12 °C.

The logarithmic mean temperature difference can be calculated from the following equation

$$\Delta T_{LMTD} = \frac{(T_{h2} - T_{c2}) - (T_{h1} - T_{c1})}{\ln\left(\frac{T_{h2} - T_{c2}}{T_{h1} - T_{c1}}\right)} \quad [9, 10] \quad (5)$$

The condenser or evaporator tubes heat transfer outer area can be calculated by the following equation

$$A_o = \Pi * d_{otube} * n_{tube} * L_{tube} * N_{pass} \quad (6)$$

Where  $d_{otube}$  is the tube outer diameter in m,  $n_{tube}$  is the tubes number,  $L_{tube}$  is the tube length in m, assuming that it doesn't exceed 1m with single pass and  $N_{pass}$  is the number of tube passes.

The condenser or evaporator tubes area can be calculated by the following equation

$$A_{tube} = \frac{\Pi}{4} d_{tube}^2 * n_{tube} \quad (7)$$

The cooling or chilled water velocity can be calculated by the following equation

$$v = \frac{\dot{m}}{\rho * A_{tube}} \quad (8)$$

Where  $\rho$  is the chilled water density in  $kg/m^3$ .

The condenser or evaporator shell diameter can be calculated by the following equation

$$D_{shell} = 0.637 \sqrt{\frac{CL}{CPT}} \sqrt{\frac{A_o (PR)^2 d_{otube}}{L_{tube}}} \quad [9] \quad (9)$$

Where CL, CLP and PR are tube layout constant, shell constant and pitch ratio respectively.

The hydraulic diameter of the condenser or evaporator tubes can be calculated by the following equation

$$D_H = 4 \left[ \frac{(Pitch)^2 - \frac{\Pi}{4} d_{otube}^2}{\Pi d_{otube}} \right] \quad [9] \quad (10)$$

The overall heat transfer coefficient of the condenser or evaporator tubes can be calculated by the following equation

$$U = \frac{1}{\frac{d_{otube}}{d_{tube} h_i} + \frac{d_{otube} * \ln\left(\frac{d_{otube}}{d_{tube}}\right)}{2k_{tube}} + \frac{1}{h_o}} \quad [9,10] \quad (11)$$

\*For shell side:  $Nu = 0.36 * Re^{0.55} * Pr^{1/3}$  [9, 10] (12)

$$Re = \frac{\dot{m}_{Re f} D_H}{\mu_{Re f} \left( \frac{D_{shell} (pitch - d_{o tube}) B}{pitch} \right)} \quad [9]$$

Where B is the baffle spacing in m which equal 0.4 to 0.6 of the shell diameter.

$$h_o = Nu \frac{k_{Re f}}{D_H} \quad [9,10] \quad (13)$$

\*For tube side:

$$Nu = 3.66 + \frac{0.0668 \left( \frac{d_{tube}}{L_{tube}} Re Pr \right)}{1 + 0.04 \left( \frac{d_{tube}}{L_{tube}} Re Pr \right)^{2/3}} \quad [10] \quad (14)$$

for laminar flow

$$Nu = 0.027 * Re^{0.8} * Pr^{0.3} \quad [10] \quad (15)$$

for turbulent flow

$$h_i = Nu \frac{k_{Re f}}{d_{tube}} \quad [10] \quad (16)$$

Table 3 adsorption chillers condensers data

	R-134a	R-407c	R-507A	H <sub>2</sub> O	H <sub>2</sub> O
$\dot{Q}_{cooling}$ (kW)	5	5	5	5	15
$\dot{Q}_{cond}$ (kW)	5.517	5.3977	5.4708	5.11545	15.346
$\dot{m}_{CW}$ (kg/s)	0.131	0.1291	0.13085	0.12235	0.367
$\dot{m}_{Re f}$ (kg/s)	0.033	0.03207	0.047	0.002126	0.0063
$d_{tube}$ (m)	0.015	0.015	0.015	0.015	0.015
$n_{tube}$	22	22	22	100	250
$N_{pass}$	10	10	10	10	10
$L_{tube}$ (m)	0.827	0.85225	0.51744	0.948297	1.0351
$D_{shell}$ (m)	0.432	0.432	0.432	0.922353	1.4583

Table 4 adsorption chillers evaporators data

	R-134a	R-407c	R-507A	H <sub>2</sub> O	H <sub>2</sub> O
$\dot{Q}_{cooling}$ (kW)	5	5	5	5	15
$\dot{m}_{ChW}$ (kg/s)	0.119	0.119	0.119	0.119	0.3987
$\dot{m}_{Re f}$ (kg/s)	0.033	0.03207	0.047	0.002126	0.0063
$d_{tube}$ (m)	0.015	0.015	0.015	0.015	0.015
$n_{tube}$	20	20	20	28	70
$N_{pass}$	6	6	6	6	6
$L_{tube}$ (m)	0.867	0.87337	0.72165	0.836292	0.9412
$D_{shell}$ (m)	0.319	0.319	0.319	0.378052	0.5977

#### 4.5.2 Adsorber Design

The following table.5 containing the output data for designing the adsorber of the experimentally tested adsorption pairs for chiller with 5 kW cooling capacity, reference SorTech chiller with 15 kW cooling capacity, reference SorTech chiller with 5 kW cooling capacity and the theoretically tested adsorption pair for chiller with 5 kW cooling capacity. The designed chillers adsorber dimensions was obtained by comparing the area needed for the mass of adsorbent needed in the designed 5 kW chiller to the mass of adsorbent already contained in the tested adsorbent bed with its area. Using the same steps of chiller design that were previously mentioned in chapter three, taking into account that the mass of adsorbent in ACG and ACP adsorption bed were 139.6 g and 44.9 g respectively.

The area of the adsorption bed heat exchanger was

$$A_{H.Exc} = 0.106425 \text{ m}^2$$

The cooling capacity of the designed 5 kW adsorption chiller was

$$\dot{Q}_{ev} = 5 \text{ kW}$$

The mass flow rate of the refrigerant in the designed 5 kW adsorption chiller was

$$\dot{m}_{Re f} = \frac{\dot{Q}_{ev}}{\Delta h_{ev}} \text{ kg/s} \quad (17)$$

Where  $\Delta h_{ev}$  is the evaporator refrigerant enthalpy difference in kJ/(kg.K)

The refrigerant mass in the designed adsorption chiller was

$$m_{Ref} = \frac{\dot{m}_{Ref}}{t_{cycle}} \text{ kg} \quad (18)$$

The adsorbent mass needed in the designed adsorption chiller was

Where  $t_{cycle}$  is the adsorption-desorption cycle time in sec

Table 5 adsorption chiller adsorber design data

	R-134a / ACP	R-134a / ACP	R-407c / ACP	R-407c / ACP	R-507A / ACP	R-507A / ACP	H <sub>2</sub> O / Silica-gel	H <sub>2</sub> O / Silica-gel
$\dot{Q}_{cooling}$ (kW)	5	5	5	5	5	5	5	15
No. adsorber / chiller	2	2	2	3	3	2	2	2
$m_{asd}$ /bed (kg)	28.48	10.93	72.92	26.85	168.7	31.2	7.22	22.32
$A_{asd}$ /bed (m <sup>2</sup> )	27.1	25.9	55.6	63	128.6	73.96	50.47	151.4
Dim. (m)	0.6*	0.6*	0.6*	0.6*	0.6*	0.6*	0.6*	0.6*
	0.35*	0.35*	0.35*	0.35*	0.35*	0.35*	0.3*	0.3*
	0.26	0.31	0.68	0.78	1.6	0.9	0.3	0.9
Fin Thick. (m)	0.3	0.3	0.3	0.3	0.3	0.3	0.3	0.3
Fin Pitch (m)	5	5	5	5	5	5	2	2
No. fins	50	60	130	150	305	175	140	420
No. tubes	100	100	100	100	100	100	100	100

$$m_{ads} = \frac{m_{Ref}}{W_{ads}} \text{ kg} \quad (19)$$

Where  $W_{ads}$  is the adsorption capacity of the pair used in the designed adsorption chiller in kg/kg  
 The area of the heat exchanger adsorber of the designed adsorption chiller was

$$A_{Bed} = \frac{m_{ads} * A_{H.Exc}}{m_{Ac}} \text{ m}^2 \quad (20)$$

Number of small heat exchanger units needed for to accommodate the designed adsorption chiller was

$$N = \frac{A_{Bed}}{A_{H.Exc}} \quad (21)$$

### 2.6 Error Analysis

The adsorbed refrigerant and the adsorption capacity values are determined values as they are not measured directly. Therefore, there are errors in their values, however, the error analysis for these determined values are calculated by using the following general method for propagating uncertainties through calculations [11].

$$E_z = \sqrt{(\alpha_1 + E_1)^2 + (\alpha_2 + E_2)^2 + \dots + (\alpha_i + E_i)^2} \quad (22)$$

$$\alpha_i = \frac{\partial z}{\partial x_i} \quad (23)$$

Where  $E_i$  is the uncertainty in quantity  $x_i$  and  $z$  is the result.

The whole uncertainty analysis is presented in Tables 6 and 7.

Table 6. Error analysis of the measured parameters

Variable	Symbol	Error
Temperature	T	± 0.05 % of reading + 0.5 °C
Pressure	P	± 0.25 bar
Water flow rate	Q <sub>w</sub>	± 5 ml
Adsorption bed final mass	m <sub>Bed</sub>	± 0.1g
Adsorption bed initial mass	m <sub>initial</sub>	± 0.1g

Table 7. Error analysis of the determined parameters

Variable	Symbol	Error
Refrigerant Mass	m <sub>Ref</sub>	± 0.141361541 g or ± 1 % of the result
Adsorption Capacity	X	± 0.000124624 g g <sup>-1</sup> or ± 0.067056106 % of the result

### III. Results and discussion

For ACP / R-407c pair, Figure (3) indicates the relation between the measured adsorbent temperature inside the adsorber and water outlet from the adsorber with time in 25 °C adsorption mode. The adsorbent temperature inside the adsorber increased in the beginning of the adsorption processes, due to

condensation of refrigerant molecules inside the adsorbent pores, then its temperature is decreased due to no more refrigerant adsorbed after 8 minutes. Water outlet temperature was increased due to absorbing the heat of adsorption. At the end of the adsorption process, the pressure inside the adsorption bed reaches 2.5 bar which is nearly reaches the refrigerant charging pressure.

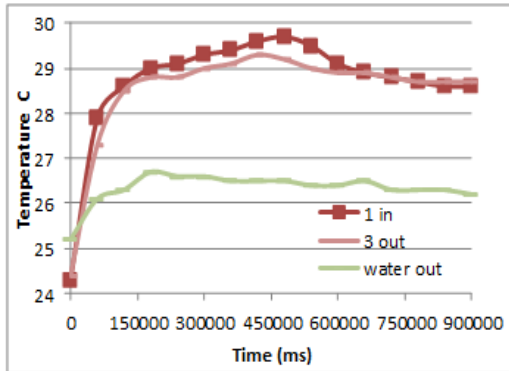


Fig. 3: Comparison between the measured adsorbent temperature inside the adsorber and water exit from the adsorber with time at 25 °C adsorption.

Figures (4) to (6) illustrate the relation between the measured adsorbent temperature inside the adsorber and water outlet from the adsorber with time, in 70 °C, 80 °C and 85 °C desorption modes after 25 °C adsorption. In all of those experiments Water outlet temperature was decreased due to rejecting the heat needed for desorption. The adsorbent temperature inside the adsorber decreased in the beginning of the desorption processes, due to evaporation of refrigerant molecules from the adsorbent pores, then its temperature is increased due to no more refrigerant desorbed after 11 minutes in case of desorption at 70 °C, 6 minutes in case of desorption at 80 °C, 3 minutes only in case of desorption at 85 °C. Therefore, when the desorption temperature increased at the same adsorption temperature, the desorption time decreased due to increase the ability of desorbing more refrigerant from the adsorbent at higher temperatures.

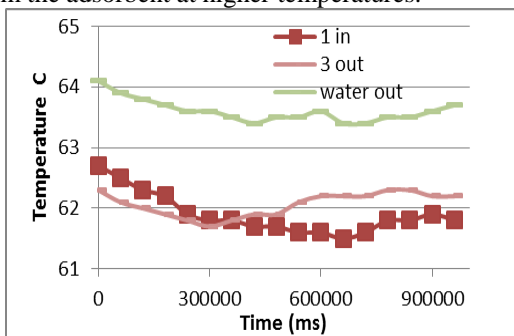


Fig. 4: Comparison between the measured adsorbent temperature inside the adsorber and water exit from the adsorber with time at 70 °C desorption after 25 °C adsorption.

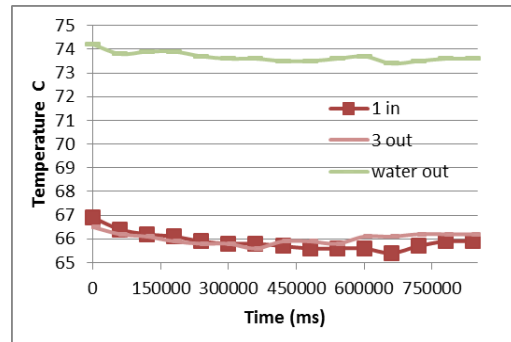


Fig. 5: Comparison between the measured adsorbent temperature inside the adsorber and water exit from the adsorber with time at 80 °C desorption correspondence to 25 °C adsorption case.

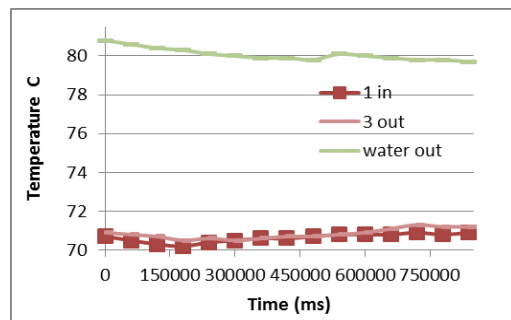


Fig. 6: Comparison between the measured adsorbent temperature inside the adsorber and water exit from the adsorber with time at 85 °C desorption after 25 °C adsorption.

Figure (7) indicates the relation between the measured adsorbent temperature inside the adsorber and water outlet from the adsorber with time in 30 °C adsorption mode. The adsorbent temperature inside the adsorber increased in the beginning of the adsorption processes, due to condensation of refrigerant molecules inside the adsorbent pores, then its temperature is decreased due to no more refrigerant adsorbed after 4 minutes. Water outlet temperature was increased due to absorbing the heat of adsorption. At the end of the adsorption process, the pressure inside the adsorption bed reaches 2.45 bar which is nearly reaches the refrigerant charging pressure.

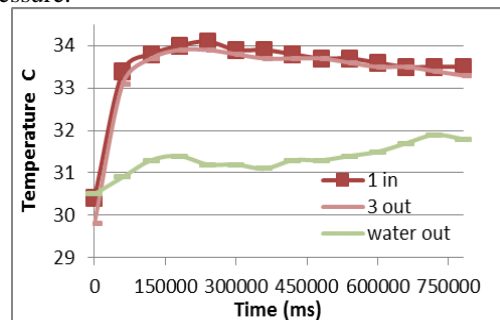


Fig. 7: Comparison between the measured adsorbent temperature inside the adsorber and water exit from the adsorber with time at 30 °C adsorption.

Figure (8) illustrates the relation between the measured adsorbent temperature inside the adsorber and water outlet from the adsorber with time, in 85 °C desorption mode after 30 °C adsorption. In this experiment the adsorbent temperature inside the adsorber decreased in the beginning of the desorption processes, due to evaporation of refrigerant molecules from the adsorbent pores, then its temperature is increased due to no more refrigerant desorbed after 3 minutes. Water outlet temperature was decreased due to rejecting the heat needed for desorption.

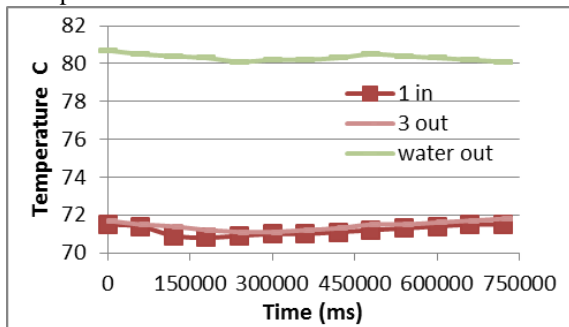


Fig. 8: Comparison between the measured adsorbent temperature inside the adsorber and water exit from the adsorber with time at 85 °C desorption correspondence to 30 °C adsorption case.

Figure (9) indicates the relation between the measured adsorbent temperature inside the adsorber and water outlet from the adsorber with time in 35 °C adsorption mode. The adsorbent temperature inside the adsorber increased in the beginning of the adsorption processes, due to condensation of refrigerant molecules inside the adsorbent pores, then its temperature is decreased due to no more refrigerant adsorbed after 3 minutes. Water outlet temperature was increased due to absorbing the heat of adsorption. At the end of the adsorption process, the pressure inside the adsorption bed reaches 2.45 bar which is nearly reaches the refrigerant charging pressure.

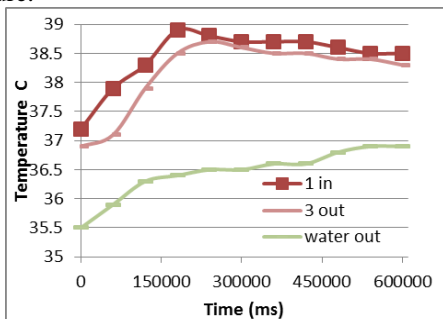


Fig. 9: Comparison between the measured adsorbent temperature inside the adsorber and water exit from the adsorber with time at 35 °C adsorption.

Figure (10) illustrates the relation between the measured adsorbent temperature inside the adsorber

and water outlet from the adsorber with time, in 85 °C desorption modes after 35 °C adsorption. In this experiment the adsorbent temperature inside the adsorber decreased in the beginning of the desorption processes, due to evaporation of refrigerant molecules from the adsorbent pores, then its temperature is increased due to no more refrigerant desorbed after 4 minutes. Water outlet temperature was decreased due to rejecting the heat needed for desorption.

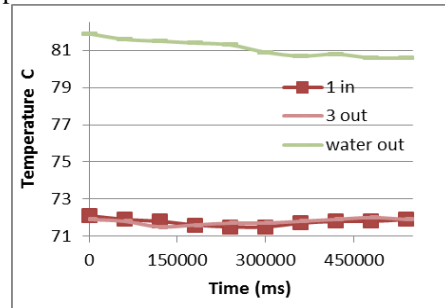


Fig. 10: Comparison between the measured adsorbent temperature inside the adsorber and water exit from the adsorber with time at 85 °C desorption after 35 °C adsorption.

Figure (11) indicates the relation between the measured adsorbent temperature inside the adsorber and water outlet from the adsorber with time in 50 °C adsorption mode. Water outlet temperature was increased due to absorbing the heat of adsorption. The adsorbent temperature inside the adsorber increased in the beginning of the adsorption processes, due to condensation of refrigerant molecules inside the adsorbent pores, then its temperature is decreased due to no more refrigerant adsorbed. Due to the increase in adsorption temperature, a small amount of refrigerant adsorbed quickly. At the end of the adsorption process, the pressure inside the adsorption bed reaches 2.3 bar which is nearly reaches the refrigerant charging pressure.

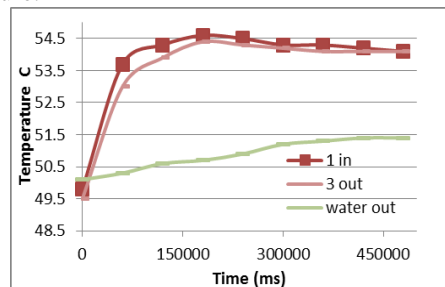


Fig. 11: Comparison between the measured adsorbent temperature inside the adsorber and water exit from the adsorber with time at 50 °C adsorption.

Figure (12) illustrates the relation between the measured adsorbent temperature inside the adsorber and water outlet from the adsorber with time, in 85 °C desorption modes after 50 °C adsorption. In this

experiment the adsorbent temperature inside the adsorber decreased in the beginning of the desorption processes, due to evaporation of refrigerant molecules from the adsorbent pores, then its temperature is increased due to no more refrigerant desorbed after 4 minutes. Water outlet temperature was decreased due to rejecting the heat needed for desorption.

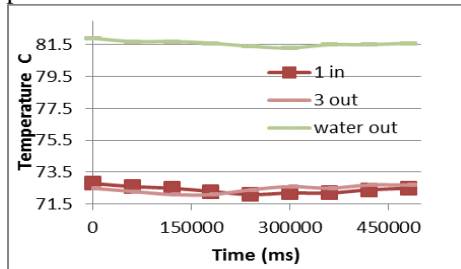


Fig. 12: Comparison between the measured adsorbent temperature inside the adsorber and water exit from the adsorber with time at 85 °C desorption correspondence to 50 °C adsorption case.

Table (8) illustrates the operation and switching processes for two complete cycles of a 3-bed adsorption chiller equipped with activated carbon powder-R-407c pair, using the optimum adsorption and desorption times of this pair, which obtained at 25 °C adsorption mode to be 8 minutes and at 85 °C desorption mode to be 3 minutes. In this case using three beds is suitable for these values of optimum time because the adsorption time is more than twice the desorption time.

Table 8 The operation processes of 3-bed system with activated carbon powder-R-407c pair

Time (min)	Bed I	Bed II	Bed III
0	Desorption	---	---
3	Adsorption	Desorption	---
6	Adsorption Continued	Adsorption	---
8	Adsorption Continued	Adsorption Continued	Desorption
11	Desorption	Adsorption Continued	Adsorption
14	Adsorption	Desorption	Adsorption Continued
17	Adsorption Continued	Adsorption	Adsorption Continued
19	Adsorption Continued	Adsorption Continued	Desorption
22	Desorption	Adsorption Continued	Adsorption

Figure 13 illustrates the relation between the adsorption capacity of the all tested pairs (ACP/R-134a, ACP/R-407c, ACP/R-507A, ACG/R-507A, ACG/R-407c and ACG/R-134a) at different

adsorption temperatures. As shown in the figure, the adsorption capacity decreased with increase the adsorption temperature. From the measured data the following results shown in Fig. (13) are obtained. The maximum adsorption capacity of ACP/R-134a pair was 0.8352 kg kg<sup>-1</sup> at 25 °C and became 0.4343 kg kg<sup>-1</sup> at 25 °C for ACP/R-407c pair. While it is 0.3163 kg kg<sup>-1</sup> at 25 °C for ACP/R-507A pair. Also, the results showed that the maximum adsorption capacity is 0.2006 kg kg<sup>-1</sup> at 25 °C for ACG//R-507A pair, 0.1583 kg kg<sup>-1</sup> at 25 °C for ACG//R-407c pair and 0.4986 kg kg<sup>-1</sup> at 25 °C for ACG//R-134a. The main obtained results for all pairs is that, at adsorption temperature of 25 °C the maximum adsorption capacity is found to be 0.8352 kg kg<sup>-1</sup> for activated carbon powder with R-134a and the minimum adsorption capacity found to be 0.1583 kg kg<sup>-1</sup> for activated carbon granules with R-407c. While, at adsorption temperature of 50 °C the maximum adsorption capacity is found to be 0.3207 kg kg<sup>-1</sup> for activated carbon powder with R-134a and the minimum adsorption capacity found to be 0.0609 kg kg<sup>-1</sup> for activated carbon granules with R-407c. It can be indicated from the figure that for the same refrigerant, the activated carbon powder adsorbent had higher sorption ability than the granular activated carbon adsorbent, this is due to the high surface area of the activated carbon powder adsorbent. Also, the adsorption capacity of all pairs is decreased by increasing the adsorption temperature, due to decreasing the sorption ability by increasing the adsorption temperature.

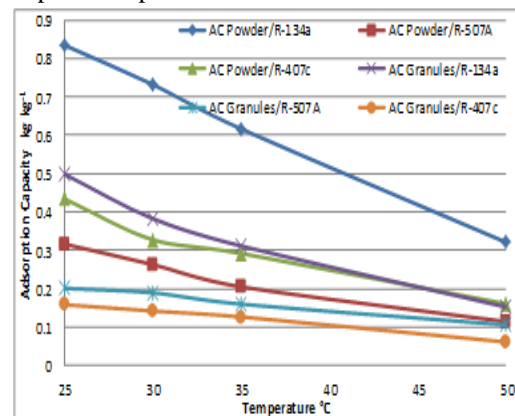


Fig. 13: Adsorption capacity of the whole six adsorption pairs with respect to the adsorption temperature.

#### IV. CONCLUSIONS

This study is experimentally targeting to develop effective in heat and mass transfer processes for the adsorbate to obtain applicable adsorption capacity data. This is done by using fin and tube heat exchanger and the adsorbate is stucked over its surface and located at the core of the adsorber. This is to estimate experimentally the maximum adsorption

capacity for six different adsorption refrigeration working pairs. The pairs are ACP/R-134a, ACP/R-407c, ACP/R-507A, ACG/R-507A, ACG/R-407c and ACG/R-134a, at different adsorption temperatures of 25, 30, 35 and 50 °C. The following is concluded from the results:

At adsorption temperature of 25 °C the maximum adsorption capacity is found to be 0.8352 kg kg<sup>-1</sup> for activated carbon powder with R-134a and the minimum adsorption capacity found to be 0.1583 kg kg<sup>-1</sup> for activated carbon granules with R-407c. While, at adsorption temperature of 50 °C the maximum adsorption capacity is found to be 0.3207 kg kg<sup>-1</sup> for activated carbon powder with R-134a and the minimum adsorption capacity found to be 0.0609 kg kg<sup>-1</sup> for activated carbon granules with R-407c.

As the adsorption temperature increased, the adsorption rate decreased.

For the same refrigerant, the activated carbon powder adsorbent had higher sorption ability than the granular activated carbon adsorbent, this is due to its high surface area.

The ACP/R-134a pair is highly recommended to be used as adsorption refrigeration working pair because of its higher maximum adsorption capacity than the other tested pairs, to produce an adsorption refrigeration system that is compact, efficient, reliable and long life.

Activated carbon granules/R-134a and activated carbon powder/R-134a 5 kW chillers are the most compact chiller components among the whole tested pairs, as their shell and tube condensers dimension are 0.83m for tubes length and 0.43m shell diameter, their shell and tube evaporators dimension are 0.87m for tubes length and 0.32m shell diameter and their fin and tube adsorbers dimension are 0.6m\*0.35m\*0.26m for activated carbon granules/R-134a chiller and 6m\* 0.35m\*0.31m for activated carbon powder/R-134a chiller.

#### ACKNOWLEDGEMENT

The first author would like to acknowledge Ministry of Higher Education (MoHE) of Egypt for providing a scholarship to conduct this study as well as the Egypt Japan University of Science and Technology (E-JUST) for offering the facility and tools needed to conduct this work.

#### REFERENCES

- [1] Dieng, A.O., Wang, R.Z., 2001. Literature review on solar adsorption technologies for ice-making and air conditioning purposes and recent developments in solar technology. *Ren. Sus. Energy Rev.* 5, 313–342.
- [2] Habib, K., Saha, B. B., Chakraborty, A., Koyama, S., Srinivasan, K., 2011. Performance evaluation of combined

adsorption refrigeration cycles. *Int. J. Refrigeration* 34, 129-137.

- [3] Askalany, A. A., Salem, M., Ismail, I.M. , Ali, A H H., Morsy, M.G., 2012a. A review on adsorption cooling systems with adsorbent carbon. *Ren. Sus. Energy Rev.* 16, 493– 500.
- [4] Solmus, I. , Rees, D. A. S., Yamali. C., Baker, D., Kaftanoglu, B., 2012. Numerical investigation of coupled heat and mass transfer inside the adsorbent bed of an adsorption cooling unit. *Int. J. Refrigeration* 35, 652-662.
- [5] Askalany, A. A., Salem, M., Ismail, I.M., Ali, A. H. H., Morsy, M.G., 2012b. Experimental study on adsorption-desorption characteristics of granular activated carbon/R134a pair. *Int. J. Refrigeration* 35, 494–498.
- [6] Shmroukh, A. N., Ali, A. H. H., Abel-Rahman, A. K., 2013. Adsorption refrigeration working pairs: The state-of-the-art in the application. *International Conference on Fluid Mechanics, Heat Transfer and Thermodynamics*. Paris.
- [7] Ali, A. H. H., Hanaoka, Y., 2002. Experimental study on laminar flow forced-convection in a channel with upper V-corrugated plate heated by radiation. *Int. J. Heat Mass Trans.* 45, 2107–2117.
- [8] Dincer, I., Kanoglu, M., 2010. *Refrigeration Systems and Applications*, second ed., A John Wiley and Sons, Ltd.
- [9] Sadik Kakaç, Hongtan Liu. *Heat Exchangers: Selection, Rating, and Thermal Design*. CRC Press 2002, Second Edition.
- [10] Incropera. *Fundamentals of heat and mass transfer*. Sixth Edition, John Wiley & sons, Inc. 2007.
- [11] Taylor, John R., 1997. *Error Analysis: The study of uncertainties in physical measurements*, second ed. University Science Books.